THE JOURNAL OF PHYSICAL CHEMISTRY B

Article

pubs.acs.org/JPCB

G-Quadruplexes from Human Telomeric DNA: How Many Conformations in PEG Containing Solutions?

Luigi Petraccone,*[,†] Anna Malafronte,[†] Jussara Amato,[‡] and Concetta Giancola[†]

[†]Dipartimento di Chimica "P. Corradini", Via Cintia, Università "Federico II" di Napoli, 80126, Naples, Italy

[‡]Dipartimento di Chimica delle Sostanze Naturali, Via D. Montesano 49, Università "Federico II" di Napoli, 80131, Naples, Italy

Supporting Information

ABSTRACT: G-quadruplex structures are an attractive target for the development of anticancer drugs, as their formation in human telomere induces a DNA damage response followed by apoptosis in cancer cells. However, the development of new anticancer drugs by means of structural-based drug design is hampered by a lack of accurate information on the exact G-quadruplex conformation adopted by the human telomeric DNA under physiological conditions. Several groups reported that, in a molecular crowded, cell-like environment, simulated by polyethylene glycol (PEG), the human telomeric DNA adopts the parallel G-quadruplex conformation. These studies have suggested that 40% (w/v) PEG concentration induces complete structural conversion from the other known human telomeric G-quadruplex conformations to the parallel G-quadruplex, thus simplifying the high structural polymorphism existing in the absence of PEG. In this study, we demonstrate that the structural conversion to the parallel G-quadruplex is not a complete reaction at physiological temperature. We report a complete kinetic and thermodynamic characterization of the conformational transitions involving the $(TTAGGG)_4TT$ and $(TTAGGG)_8TT$ human telomeric DNA sequences in K^+ solution containing PEG. Our data show that the hybrid-type and parallel conformations coexist at equilibrium in the presence of PEG at physiological temperature and the degree of the quadruplex interconversion depends on the PEG molecular weight. Further, we find that telomeric DNA folds in the parallel quadruplex in the seconds time scale, a much larger time scale than the one reported for the hybrid quadruplex folding (~ms). The whole of our data allow us to predict the relative amount of each G-quadruplex conformation as a function of temperature and time. The effect of other crowding agents like Ficoll 400 and glycerol on the quadruplex interconversion has been also explored.

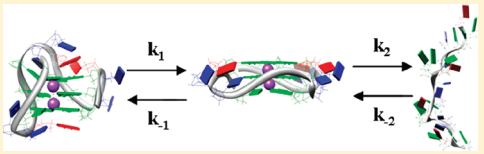

INTRODUCTION

Human telomeric DNA contains thousands of tandem repeats of the sequence TTAGGG that terminates at the 3′-end as single-stranded G-rich overhangs of 100−200 nt.[1,2] The human telomeric overhangs can fold into G-quadruplex structures stabilized by consecutive G-tetrads connected by loops.[3] Several cell-based studies have shown that folding of the telomeric G-rich single strand into a quadruplex structure alters the structure of the telomere, inducing a DNA damage response followed by apoptosis in cancer cells.[4,5] For this reason, G-quadruplex structures are currently an attractive target for development of anticancer drugs.[4,6] However, the development of new anticancer drugs by means of structural-based drug design is hampered by the lack of accurate information on the exact G-quadruplex conformation adopted by the human telomeric DNA under physiological conditions.

Extensive structural investigations have been carried out by NMR on human telomeric sequences containing four G-tracts in physiological K^+ solution.[7−11] The majority of the explored sequences form the hybrid-1 or hybrid-2 structures (or a mix of both of them). These two topologies, also named (3 + 1), have three G-tracts oriented in one direction and the fourth in the opposite direction, but they differ in the order of the loop arrangements.[8] The $GGG(TTAGGG)_3$ sequence, a particular truncation of the human telomeric DNA, has been shown to form an antiparallel basket type form (called Form-3) containing just two G-quartets.[11] The crystal structure of the human telomeric quadruplex in K^+ differs from the NMR structures and has all four G-tracts parallel and connected by three propeller loops.[12] Although the parallel fold seems not to be the predominant conformation in dilute solution,[13] several groups reported that in molecular crowding conditions, simulated by polyethylene glycol (PEG), the human telomeric DNA adopts the parallel G-quadruplex conformation.[13−17] Since molecular crowding is the typical condition in cells,[18] these results have raised much attention and have been used to suggest that the parallel quadruplex is biologically relevant. However, recently, doubts have been raised on the use of PEG to simulate crowding conditions,[19] as it could interact with macromolecules rather than being an inherent partner.[20] Other authors have suggested that the PEG acts on DNA more as a dehydrating agent rather than as a molecular crowding agent.[21] For these reasons, careful considerations are required when using agents such as PEG to mimic molecular crowding. Besides this, the detailed kinetics and thermodynamics of the

Received: September 22, 2011
Revised: January 19, 2012
Published: January 23, 2012

dx.doi.org/10.1021/jp209170v | J. Phys. Chem. B 2012, 116, 2294−2305

structural conversion to the parallel G-quadruplex induced by PEG is not fully understood.

In most studies on the conformational changes induced by PEG, the DNA samples are subjected to an annealing procedure (heating of the sample above 90 °C and slow cooling at room temperature) to force the formation of the parallel topology;[14,17,22,23] this procedure does not correspond to the physiological conditions (the cellular temperature is approximately constant at 37 °C). Further, the human telomeric sequences employed are short human telomeric sequences (in the range 21−26 nt) able to fold into a single quadruplex structure.[14,23] To properly search for the physiologically relevant structures of the telomeric DNA, the ability of longer human telomeric sequences (eight or more repeats) to form consecutive quadruplex units needs to be taken into account.[24−26]

Very recently, the kinetic constant for the hybrid to parallel transformation has been determined for some human telomeric sequences in the presence of PEG.[16,27] These studies suggest that the transformation is complete and irreversible at physiological temperature. However, they generally neglect the contribution of the reverse reaction (parallel to hybrid transformation), thus leading to a possible underestimate of the amount of the remaining hybrid conformation at the thermodynamic equilibrium. Further, no detailed information exists on the formation of the parallel or hybrid conformation starting from the unfolded single strand in the presence of PEG. This information could be very important to determine which quadruplex conformation is relevant in the time scale of the biochemical processes.

In this study, we explored the conformational transitions involving the $(TTAGGG)_4TT$ and $(TTAGGG)_8TT$ human telomeric sequences in K^+ solution and in the presence of 40% (w/v) PEG200 by means of CD and fluorescence spectroscopy, SVD analysis, and gel electrophoresis. The two sequences $(TTAGGG)_4TT$ and $(TTAGGG)_8TT$ were selected, as they have been previously well characterized. The $(TTAGGG)_4TT$ sequence forms a hybrid quadruplex in K^+ solution,[10] whereas the $(TTAGGG)_8TT$ sequence forms two consecutive hybrid quadruplexes and could be a better model of the long human telomeric overhang than the $(TTAGGG)_4TT$ short human telomeric sequence.[28] The kinetics of the hybrid−parallel quadruplex interconversion and the folding/unfolding process of the parallel quadruplex were explored in a wide range of temperature.

The whole of our data allowed us to determine the relative populations of the quadruplex conformations in K^+ solution. In contrast with previous studies,[16,27] we found that the hybrid-to-parallel interconversion is not a complete reaction at 37 °C and a significant amount of hybrid conformation is present at thermodynamic equilibrium. We also explored the effects of the molecular weight of PEG and of other crowding agents of different nature (Ficoll 400 and glycerol) on the hybrid−parallel equilibrium. Further, we determined for the first time the folding kinetics of the DNA single strand in the parallel quadruplex, finding that telomere DNA folds in this quadruplex structure in the seconds time scale, a much larger time scale than the one (∼ms) reported for the folding of the hybrid quadruplex.[29,30]

EXPERIMENTAL METHODS

DNA Sample Preparation. The $(TTAGGG)_8TT$ and $(TTAGGG)_4TT$ oligonucleotides and the fluorescence analogues of the $(TTAGGG)_8TT$ were purchased from the Primm Company (Milan, Italy); poly(ethylene glycol) of average molecular weight 200 (PEG200), 3400 (PEG3400), and 10000 (PEG10000) and Ficoll 400 and glycerol were purchased from Sigma-Aldrich. Stock DNA solutions were prepared by dissolving the lyophilized compounds in a buffer solution containing 20 mM phosphate with 100 mM KCl, 0.1 mM EDTA, at pH 7.0. The stock solutions were then heated at 95 °C for 5 min and then slowly cooled to room temperature. The concentration of oligonucleotides was determined by UV adsorption measurements at 90 °C using molar extinction coefficient values $\varepsilon_{(260\ nm)}$ of 261200 and 505600 $M^{-1}\ cm^{-1}$ for $(TTAGGG)_4TT$ and $(TTAGGG)_8TT$, respectively. The molar extinction coefficients were calculated by the nearest neighbor model.[31] For all the experiments, the stock solutions were diluted by buffer and PEG200 to achieve the desired DNA and PEG200 concentrations.

CD Spectroscopy. CD spectra were recorded with a Jasco J-715 spectropolarimeter equipped with a Peltier-type temperature control system (model PTC-348WI), and calibrated with an aqueous solution of 0.06% d-10-(1)-camphorsulfonic acid at 290 nm. The molar ellipticity $[\theta]$ (deg $cm^2\ dmol^{-1}$) was calculated from the equation $[\theta] = [\theta]_{obs}/10 \times l \times C$, where $[\theta]_{obs}$ is the ellipticity (mdeg), C is the oligonucleotide molar concentration, and l is the optical path length of the cell (cm). The cell with 0.1 and 1.0 cm path length and oligonucleotide concentration in the range 2−48 μM was used to record CD spectra between 220 and 320 nm. A scan speed of 50 nm/min, 0.5 nm data pitch, and 2 nm bandwidth were used to acquire the data. The scan of the buffer was subtracted from the scan of each sample.

CD melting profiles were collected following the CD signal at 264 and/or at 300 nm in a 15−110 °C temperature range at scan rates of 0.3, 1.0, and 3.0 °C/min. Unless otherwise stated, the samples were equilibrated at 20 °C for a few minutes after PEG200 was added before starting the temperature scan.

CD Kinetic Measurements. Kinetic experiments were carried out by following the CD signal at 264 and/or at 300 nm with increasing time and in the selected temperature range depending on the kinetics explored. The concentration of the oligonucleotides were in the range 2−48 μM depending on the DNA sequence and the path length of the cell (0.1 or 1.0 cm) employed. Unless otherwise stated, all experiments were carried out in a buffer solution containing 20 mM phosphate with 100 mM KCl, 0.1 mM EDTA, 40% PEG200, at pH 7.0. The rate constants were obtained by fitting the experimental kinetic curves to a specific kinetic model depending on the particular process explored (see below). Activation energies were obtained by the linear fit of the plots of the logarithm of the rate constants as a function of $1/T$.

(a). Hy−P and P−Hy Transition. The kinetics of the transition between the hybrid quadruplex (Hy) and the parallel (P) quadruplex and the reverse transition were explored in the 37−55 °C temperature range where other reactions can be neglected (see the Results and Discussion section). Assuming that both the Hy-to-P and P-to-Hy reactions occur, the rate equation for the change in Hy concentration can be written as

$$\frac{d[Hy]}{dt} = -k_1[Hy] + k_{-1}[P] \quad (1)$$

On the right-hand side, the first term represents the hybrid-to-parallel quadruplex transformation and the second term represents the reverse transformation. k_1 and k_{-1} are the

dx.doi.org/10.1021/jp209170v | J. Phys. Chem. B 2012, 116, 2294−2305

kinetic constants for the direct and inverse reactions, respectively. If the P conformation is not present at the beginning of the reaction, eq 1 becomes

$$\frac{d[Hy]}{dt} = -k_1[Hy] + k_{-1}([Hy]_0 - [Hy]) \quad (2)$$

where $[Hy]_0$ is the initial concentration of Hy. The concentration of the Hy quadruplex was assumed directly proportional to the CD signal at 300 nm, as the parallel folding and the unstructured single strand do not significantly contribute to the CD signal at this wavelength.[32] In this assumption and solving eq 2, it can be shown that the CD signal variation at 300 nm over time is given by

$$CD_t^{300nm} = CD_0^{300nm}\frac{k_{-1} + k_1 e^{-(k_1+k_{-1})t}}{k_{-1} + k_1} \quad (3)$$

where CD_0^{300nm} is the initial CD signal value (at 300 nm) immediately after addition of PEG200 (it corresponds to the 100% Hy conformation). The kinetic constants were obtained by fitting the experimental plots of the CD signal at 300 nm with eq 3.

(b). P–S and S–P Transition. The kinetics of the parallel (P) to single strand (S) transition and the kinetics of the parallel quadruplex folding from the unfolded single strand were explored by following the CD signal at 264 nm over time in the 60–95 °C temperature range. Assuming that (in the explored temperature range) both the reactions contribute to the variation of the P concentration, the rate equation for the change in P concentration is given by

$$\frac{d[P]}{dt} = -k_2[P] + k_{-2}[S] \quad (4)$$

where k_2 and k_{-2} are the kinetic constants for the direct and inverse reactions, respectively. Above 60 °C, the CD signal at 264 nm was assumed proportional to the P concentration as the population of the Hy form is negligible (see the Results and Discussion section) and the spectrum of the unfolded single strand does not have acontribution at 264 nm.[32] In analogy with the derivation of eq 3, it can be shown that the CD signal variation at 264 nm over time is given by the equation

$$CD_t^{264nm} = CD_0^{264nm}\frac{k_{-2} + k_2 e^{-(k_2+k_{-2})t}}{k_{-2} + k_2} \quad (5)$$

where CD_0^{264nm} is the CD signal at 264 nm of the sample equilibrated at 60 °C (it corresponds to the maximum of P concentration). Before each measurement, the sample was equilibrated at 60 °C for 10 min (to have the maximum of P conformation as the starting state) before fast heating at a given temperature. The kinetic constants at different temperatures were obtained by fitting the experimental plots of the CD signal at 264 nm with eq 5.

SVD Analysis. The CD spectra versus temperature and versus time were analyzed by singular value decomposition (SVD) to determine the number of significant spectral species involved in the observed CD variation.[33−35] SVD is a method from linear algebra for factoring a matrix.[34] Briefly, the matrix of the CD spectra A is decomposed by the SVD method into the product of three matrices:

$$A = USV^t \quad (6)$$

The matrix U contains the basis spectra, S is a diagonal matrix that contains the singular values, and V is a matrix containing the coefficient vectors. Examination of the magnitude of the singular values and of the autocorrelation functions of the basis spectra and the coefficient vectors permits one to determine the minimum number of component spectra required to describe the data within the random noise. By plotting the singular values versus the component number, it is possible to determine which (and how many) singular values deviate from the noise within the data. The value of the autocorrelation function is a measure of the smoothness between adjacent row elements. Values near 1 indicate slow variation from row to row, or "signal". A value of the autocorrelation function of 0.8 corresponds to a signal-to-noise ratio of 1, and autocorrelation values higher than 0.8 for both the U and V matrices are usually selected as a cutoff criterion for accepting a significant spectral species.[34,36] An additional indication of the number of significant spectral species is provided by the evaluation of the contribution of each singular value to the total variance in singular values. The relative variance (RV) of each singular value is given by

$$RV = \frac{S_i^2}{\sum_i S_i^2} \quad (7)$$

where S_i^2 is the square of the singular value. Only the significant singular values will sum to contribute to >0.99 of the total variance.[33]

Steady-State Fluorescence Experiments. Fluorescence spectra of the 2-AP-substituted oligonucleotides were collected with a JASCO model FP-750 fluorometer equipped with a Peltier temperature controller. Oligonucleotides were excited at 305 nm with a slit width of 5 nm and emission spectra collected from 320 to 460 nm. A sealed quartz cuvette with a path length of 1 cm was used. All measurements were performed in the presence of 40% (w/v) PEG200, and the oligonucleotide concentration was 2 μM for all the experiments.

Gel Electrophoresis. Native gel electrophoresis experiments were performed on 15% polyacrilamide gel (29:1 acrylamide:bisacrylamide ratio) containing 40% (w/v) PEG 200 and 100 mM KCl. Gels were run at 4 °C and 60 V for 5 h in 1× TBE (Tris-Borate-EDTA, from BIORAD) running buffer supplemented with 100 mM KCl. Oligonucleotide samples were prepared at 30 μM initial concentration in a buffer having the appropriate composition. Glycerol was added (10% final) to facilitate sample loading in the wells. The gels were stained with SYBR Green I Nucleic Acids dye (from Sigma) and scanned using the GEL-DOC XR (from BIORAD). The quantitative analysis of the bands was performed by using the volume tool of the Quantity One software.

RESULTS AND DISCUSSION

Temperature Induced Conformational Changes of Human Telomeric Quadruplex in PEG Containing Solutions. CD spectra of $(TTAGGG)_4TT$ and $(TTAGGG)_8TT$ in 40% PEG200 (Figure 1) before the annealing procedure are almost superimposable to the corresponding spectra obtained in the absence of PEG200, showing a positive peak at 290 nm, a shoulder at 270 nm, and a negative peak at about 240 nm. This demonstrates that, before heating of the samples, the $(TTAGGG)_4TT$ and $(TTAGGG)_8TT$ quadruplex structures are similar to the corresponding structures formed in dilute solution. Under

dx.doi.org/10.1021/jp209170v | J. Phys. Chem. B 2012, 116, 2294–2305

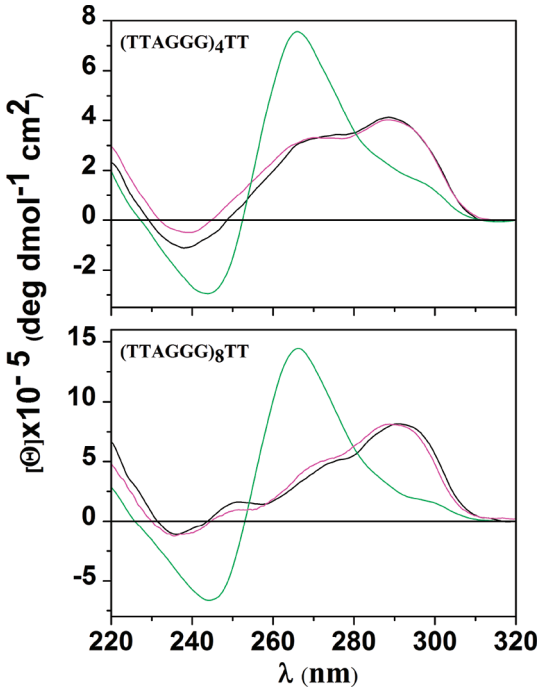

Figure 1. CD spectra of $(TTAGGG)_4TT$ and $(TTAGGG)_8TT$ recorded at 20 °C in the absence of PEG200 (black line) and in the presence of PEG200 before (magenta line) and after (green line) heat denaturation and renaturation of the DNA samples. All the solutions contain 20 mM phosphate with 100 mM KCl, 0.1 mM EDTA, at pH 7.0.

these conditions, $(TTAGGG)_4TT$ forms the hybrid-2 conformation,[8,10] whereas $(TTAGGG)_8TT$ forms two consecutive hybrid-type quadruplexes.[28] After annealing of the sample, the CD spectrum of both sequences shows a maximum at 264 nm and a minimum at 243 nm. This spectral change has been attributed by many authors to the formation of the parallel quadruplex of the human telomeric DNA.[14,16,27,37] All together, these observations indicate that there is a large energetic barrier for the conformational transition between the initial hybrid-type conformation of both $(TTAGGG)_8TT$ and $(TTAGGG)_4TT$ and the final parallel conformation but do not provide any detailed information on the magnitude of this energy barrier and on the other relevant kinetic and thermodynamic aspects of the conformational transition. To get more insight into these temperature-induced conformational changes, we recorded CD spectra at every 2 °C in the range 24−104 °C, starting from the hybrid conformations observed at low temperature before heating of the samples. The observed spectral evolution (for both sequences) is consistent with the transition from the initial hybrid conformation (at low temperature) to the parallel conformation (prevalent at about 60 °C) and, at higher temperatures, to the unfolded single strand (Figure 2a,b and Figure S1a,b in the Supporting Information). From the plots of the CD signal at 264 nm on changing temperature, it is possible to follow both of the transitions (Figure 2c and Figure S1c in the Supporting Information). Particularly, in the range 24−60 °C, we observed an increase of the CD signal at 264 nm corresponding to the conversion of the hybrid conformation (Hy) in the parallel conformation (P), whereas in the range 60−104 °C, the CD signal decreases, indicating the formation of the unfolded single

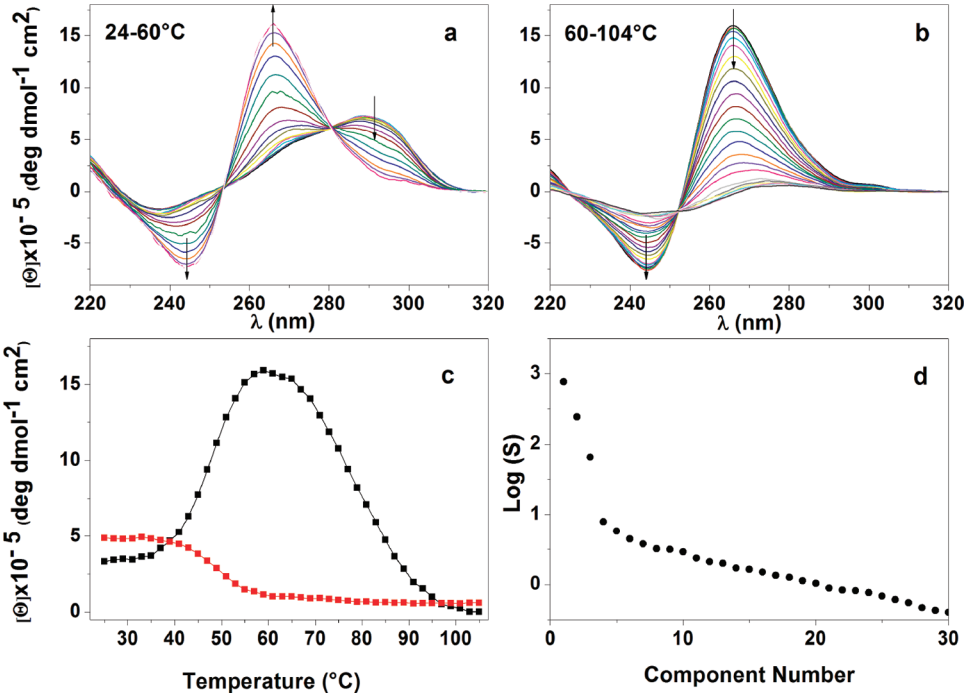

Figure 2. (a) CD spectra of $(TTAGGG)_8TT$ recorded in the range 24−60 °C and (b) 60−104 °C. The black arrows indicate the direction of the increasing temperature. CD spectra are shown every 2 °C starting from 24 °C. (c) Intensity of the molar ellipticity at 264 nm (black squares) and at 300 nm (red squares) as a function of temperature. (d) Plot of the logarithm of the first 30 singular values obtained from the SVD analysis on the wavelength versus temperature matrix constructed from CD data shown in panels a and b. All the solutions contain 20 mM phosphate with 100 mM KCl, 0.1 mM EDTA, 40% PEG200, at pH 7.0. The experiments were performed just after the PEG was added to the DNA sample without subjecting the sample to the annealing procedure.

dx.doi.org/10.1021/jp209170v | J. Phys. Chem. B 2012, 116, 2294−2305

strand (S). Interestingly, the plots of the CD signal at 300 nm (Figure 2c and Figure S1c in the Supporting Information) allow one to follow only the hybrid conformation, as the contribution of the parallel conformation is negligible at this wavelength.[32,38] The melting temperature of the first transition in the plots of the CD signal at 264 nm is close to the melting temperature derived from the plots of the CD signal at 300 nm, suggesting that it corresponds to the hybrid-to-parallel quadruplex transition (Figure 2c and Figure S1c in the Supporting Information).

To confirm that only three main spectral species (Hy, P, and S) are sufficient to describe the observed spectral variation, an SVD analysis on our CD data was performed (see the Experimental Methods section for details). The first eight singular values with the corresponding autocorrelation functions of the basis spectra (columns of *U*) and the coefficient vectors (columns of *V*) are reported in Table 1 together with the contribution of each singular value to the total variance (RV).

Table 1. Results from SVD Analysis of the CD Spectra Series on Changing the Temperature

	autocorrelation		
singular values	*U* matrix	*V* matrix	RV[a]
	$^{5'}(TTAGGG)_4TT^{3'}$		
879.493	0.9980	0.9874	0.8949
283.937	0.9966	0.9620	0.0932
99.115	0.9954	0.9438	0.0113
9.470	0.9356	0.5758	1.037×10^{-4}
5.282	0.8707	−0.08235	3.228×10^{-5}
5.181	0.8837	0.2904	3.105×10^{-5}
4.818	0.8496	0.04588	2.685×10^{-5}
4.456	0.8504	0.03998	2.297×10^{-5}
	$^{5'}(TTAGGG)_8TT^{3'}$		
773.480	0.9984	0.9911	0.90301
244.507	0.9972	0.9458	0.09024
65.416	0.9969	0.9481	0.00646
7.894	0.9769	0.5460	9.4050×10^{-5}
5.812	0.9356	0.3233	5.0995×10^{-5}
4.495	0.9655	0.1878	3.0493×10^{-5}
3.792	0.8757	0.05903	2.1708×10^{-5}
3.233	0.9750	−0.08573	1.5776×10^{-5}

[a]Relative variance of each singular value.

The magnitudes of the singular values provide the first indication of the number of significant spectral species. We found that the first three to four singular values appear to significantly deviate from the smooth, linear behavior of the remaining *S* values (Figure 2d and Figure S1d in the Supporting Information). Analysis of the magnitudes of the autocorrelation factors of the *V* and *U* matrices and of the relative variance (RV) associated with each *S* value (Table 1) reveals that three main conformations are involved in the whole melting process (a value of 0.8 for the autocorrelation factors of both the *U* and *V* matrices was selected as a cutoff criterion for accepting a significant spectral species; this value corresponds to a signal/noise ratio of 1) and that the presence of other conformations (and of their contributions to the spectral variation) is negligible.

On this basis, the observed CD melting curves can be represented as a sum of two sequential transitions, the Hy−P interconversion followed by the P melting, according to the reaction scheme shown in Scheme 1, where k_1, k_{-1} and k_2, k_{-2}

Scheme 1. Conformational Equilibria between the Hybrid (Hy), Parallel (P), and Unfolded Single Strand (S) Conformations

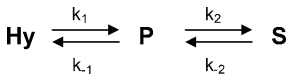

are the direct and reverse kinetic constants for the Hy−P and P−S reactions, respectively. To predict the most relevant conformation/s of human telomeric DNA under physiological conditions, all the kinetic parameters need to be known. To address this point, kinetic experiments were carried out by monitoring the CD signal at 264 or 300 nm as a function of time and in a wide range of temperatures. In the following paragraph, we showed that the two reactions, represented in the Scheme 1, can be separately investigated by appropriately choosing the temperature range and the wavelength monitored.

(a). Kinetics of the Conformational Changes of Human Telomeric DNA in the Presence of PEG200. *Hy−P: Kinetics of the Hybrid−Parallel Conformation Transition.* To study the kinetics of the Hy−P reaction and of the reverse reaction P−Hy, the DNA sequences were dissolved in K^+ buffer in the presence of PEG without preheating of the samples and CD spectra were recorded as a function of time. Figure 3a shows the CD spectra on increasing time, at 37 °C for $(TTAGGG)_8TT$. We observed that the spectral shape characteristic of the hybrid conformation disappears and the spectral shape of the parallel fold becomes more marked with increasing time. However, in the final spectrum (at equilibrium), a significant shoulder at 295 nm is still present, suggesting that the conformational change Hy−P is not complete and the reverse reaction P−Hy is not negligible at physiological temperature. Figure 3b shows the plot of the CD signal at 300 nm vs the CD signal at 264 nm with changing time for $(TTAGGG)_8TT$. The linearity of the plot strongly suggests the presence of a two-state transition between the hybrid and parallel conformations. Similar results were obtained for $(TTAGGG)_4TT$ (Figure S2, Supporting Information). Inspection of the singular values with their relative variance (RV) and of the *U* and *V* autocorrelation functions obtained from the SVD analysis performed on the wavelength versus time matrices (Table S1, Supporting Information) confirms that only two significant spectral species are involved in this conformational transition, suggesting that Hy-to-P conversion is an elementary reaction that does not involve intermediate species. Figure 3c shows the kinetic curve for the $(TTAGGG)_8TT$ quadruplex interconversion obtained by plotting the CD signal at 300 nm as a function of time at 37 °C. Similar kinetic curves were obtained for both DNA sequences in the 37−55 °C temperature range (Figures S2c and S3, Supporting Information). The CD signal at 300 nm is directly proportional to the hybrid (Hy) concentration, as the contribution of the parallel fold is negligible at this wavelength. Assuming that both Hy−P and P−Hy reactions contribute to the variation over time of the Hy concentration, the corresponding kinetic constants were obtained by fitting the kinetics curves with eq 3 (see Experimental Methods). The obtained kinetic parameters are reported in Table 2. There was a good agreement between the experimental points and the fitting curves (Figure 3c and Figures S2c and S3 in the

dx.doi.org/10.1021/jp209170v | J. Phys. Chem. B 2012, 116, 2294−2305

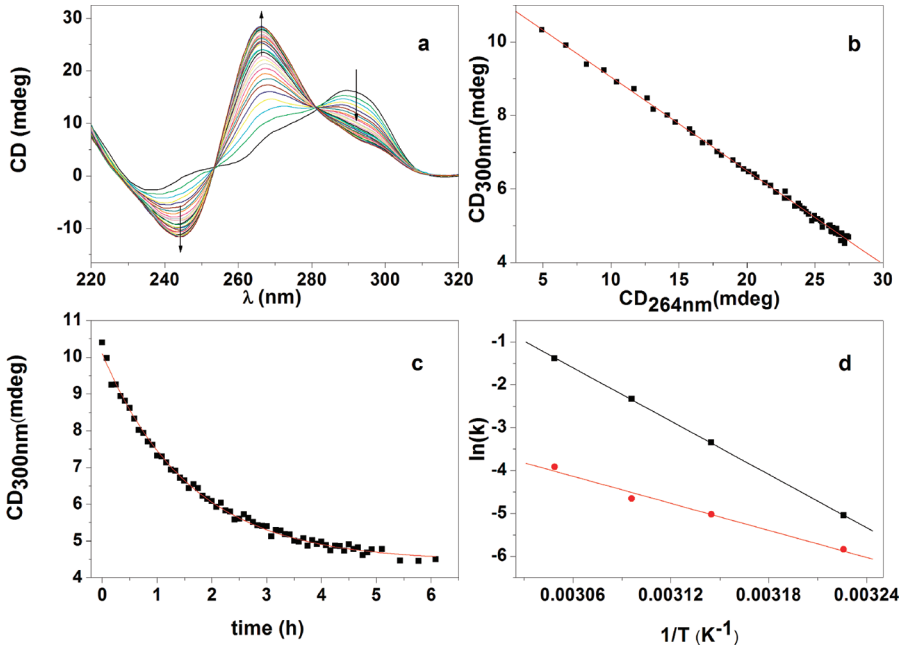

Figure 3. (a) CD spectra of $(TTAGGG)_8TT$ (2 μM) as a function of time at 37 °C in 20 mM phosphate with 100 mM KCl, 0.1 mM EDTA, 40% PEG200, at pH 7.0. The reported CD spectra were collected each 10 min; the black arrows indicate the direction of increasing time. (b) Plot of the CD intensity at 300 nm versus CD intensity at 264 nm at increasing time. (c) CD intensity at 300 nm as a function of time at 37 °C (black square) and the fitting function (red solid line). (d) Arrhenius plots for the Hy-to-P (black squares) and P-to-Hy (red circles) reactions.

Table 2. Kinetic Parameters for the Hy-to-P and P-to-Hy Reactions

T (°C)	k_1 (min^{-1})	k_{-1} (min^{-1})	K_{eq} [a]	E_a^1 (kJ mol^{-1})	E_a^{-1} (kJ mol^{-1})	ΔH^0 [b] (kJ mol^{-1})
			$(TTAGGG)_4TT$			
37	$(4.6 \pm 0.2) \times 10^{-3}$	$(3.0 \pm 0.1) \times 10^{-3}$	1.5 ± 0.1			
45	$(2.7 \pm 0.2) \times 10^{-2}$	$(6.6 \pm 0.3) \times 10^{-3}$	4.1 ± 0.1			
50	$(7.7 \pm 0.3) \times 10^{-2}$	$(1.2 \pm 0.2) \times 10^{-2}$	6.4 ± 0.2	180 ± 4	92 ± 5	88 ± 6
55	$(2.2 \pm 0.2) \times 10^{-1}$	$(2.1 \pm 0.2) \times 10^{-2}$	10.4 ± 0.2			
			$(TTAGGG)_8TT$			
37	$(6.4 \pm 0.2) \times 10^{-3}$	$(2.9 \pm 0.1) \times 10^{-3}$	2.2 ± 0.1			
45	$(3.5 \pm 0.1) \times 10^{-2}$	$(7.6 \pm 0.4) \times 10^{-3}$	4.6 ± 0.1			
50	$(9.7 \pm 0.2) \times 10^{-2}$	$(1.1 \pm 0.2) \times 10^{-2}$	8.8 ± 0.2	172 ± 4	89 ± 6	83 ± 7
55	$(2.5 \pm 0.1) \times 10^{-1}$	$(1.8 \pm 0.3) \times 10^{-1}$	13.9 ± 0.2			

[a] Computed from $K_{eq} = k_1/k_{-1}$. [b] Computed from $\Delta H^0 = E_a^1 - E_a^{-1}$.

Supporting Information), suggesting that the conformational equilibrium between Hy and P is well described by first-order reactions. The equilibrium constants ($K_{eq} = k_1/k_{-1}$) for the Hy-to-P interconversion at 37 °C were 1.5 and 2.2 for $(TTAGGG)_4TT$ and $(TTAGGG)_8TT$, respectively; these K_{eq} values correspond to up to ~30−40% of hybrid conformation (Table 2). This finding reveals that, at equilibrium, the amount of hybrid conformation is not negligible. The comparison of equilibrium constants for $(TTAGGG)_8TT$ and $(TTAGGG)_4TT$ reveals that the presence of two consecutive quadruplexes slightly favors the formation of the parallel conformation. Analysis of the Arrhenius plots (Figure 3d and Figure S2d in the Supporting Information) allowed us to determine the activation energies for the conformational changes (Table 2). The activation energies for the Hy-to-P transition are very similar for both DNA sequences, suggesting that the two quadruplex subunits in the $(TTAGGG)_8TT$ hybrid structure behave as relatively independent. From the activation energies, we calculated the enthalpy change for the Hy-to-P transformation ($\Delta H^0 = E_a^1 - E_a^{-1}$); we found for both sequences a positive enthalpy change (Table 2), revealing that interactions are lost in the hybrid-to-parallel transition.

To further check the $(TTAGGG)_8TT$ conformations in PEG on changing temperature, fluorescence experiments were carried out using $(TTAGGG)_8TT$ with 2-aminopurine (Ap) substitution at position 9, 15, 33, and 39. The first two Ap (Ap9 and Ap15) belong to one quadruplex subunit, whereas the last two Ap (Ap33 and Ap39) belong to the other quadruplex subunits (Figure S4, Supporting Information). In a previous study, some of us showed that Ap9 and Ap15 (and Ap33 and Ap39) have a higher fluorescence difference when the corresponding quadruplex subunit is in a hybrid-type conformation, whereas all of them should have similar fluorescence when the two quadruplexes are in the parallel conformation.[28] We found that the relative order of the fluorescence intensity of these residues (Figure 4, top) in the presence of PEG at 20 °C, and before heating of the sample, is similar to the one reported in the absence of PEG. This result further confirms that the starting conformation (for both of the quadruplex subunits) in the presence of PEG is the hybrid conformation observed in dilute solution. On the contrary, 2-

dx.doi.org/10.1021/jp209170v | J. Phys. Chem. B 2012, 116, 2294−2305

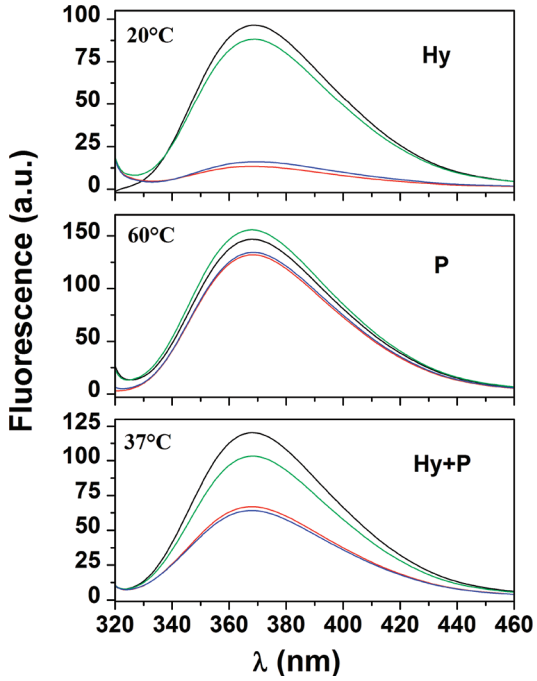

Figure 4. Fluorescence spectra of the 2-Ap residues at position 9 (black), 15 (red), 33 (green), and 39 (blue) in the $(TTAGGG)_8TT$ sequence. Spectra were recorded before heating (top), after equilibration at 60 °C for 15 min (middle), and after equilibration at 37 °C for 24 h (bottom). All solutions contain 20 mM phosphate with 100 mM KCl, 0.1 mM EDTA, 40% PEG200, at pH 7.0. The oligonucloetide concentration was 2 μM. The excitation wavelength was 305 nm.

Ap-substituted oligonucleotides show very similar fluorescence emission when equilibrated at 60 °C (Figure 4, middle), revealing the presence of a conformation with similar local environment for the four adenine residues, as expected for the parallel quadruplex fold. However, in the sample equilibrated at 37 °C for 24 h (Figure 4, bottom), the fluorescence order of the 2-Ap substituted oligonucleotides is similar to the one observed at 20 °C, suggesting that a significant amount of hybrid conformation is present at this temperature, as the contribution of the parallel fold to the fluorescence is the same for all the 2-Ap. This observation is consistent with the results of the kinetic experiments performed at 37 °C, indicating the presence of both Hy and P conformations at equilibrium. This result differs from the result reported in a previous NMR study,[16] suggesting full transformation of the hybrid form in the parallel form. A possible source of this discrepancy could be the slightly different experimental conditions or, most likely, the different sequences employed. In the previous NMR study, full transformation in the parallel fold is shown for the $TAG_3(TTAG_3)_3$ sequence, whereas we show incomplete transformation for the $(TTAGGG)_4TT$ and $(TTAGGG)_8TT$ telomeric sequences. Although this topic needs to be further explored, we think that, in the presence of a sequence dependent effect, the longer DNA sequences (as the $(TTAGGG)_8TT$ employed in this study) should be considered as more representative of the full length telomeric DNA than the short DNA sequences.

(b). P–S: Kinetics of the Parallel–Unfolded Single Strand Conformation Transition. Kinetic experiments were performed to explore the P–S and S–P reactions for $(TTAGGG)_4TT$ and $(TTAGGG)_8TT$. We showed that at 60 °C the parallel conformation becomes dominant in the presence of PEG200, whereas the hybrid conformation (and its contribution to the CD signal) is negligible. Further, the CD signal of the unfolded single strand is close to zero at 264 nm.[32] These circumstances make the CD signal at 264 nm particularly suitable to follow the parallel state folding/unfolding by choosing the temperature range appropriately. Following

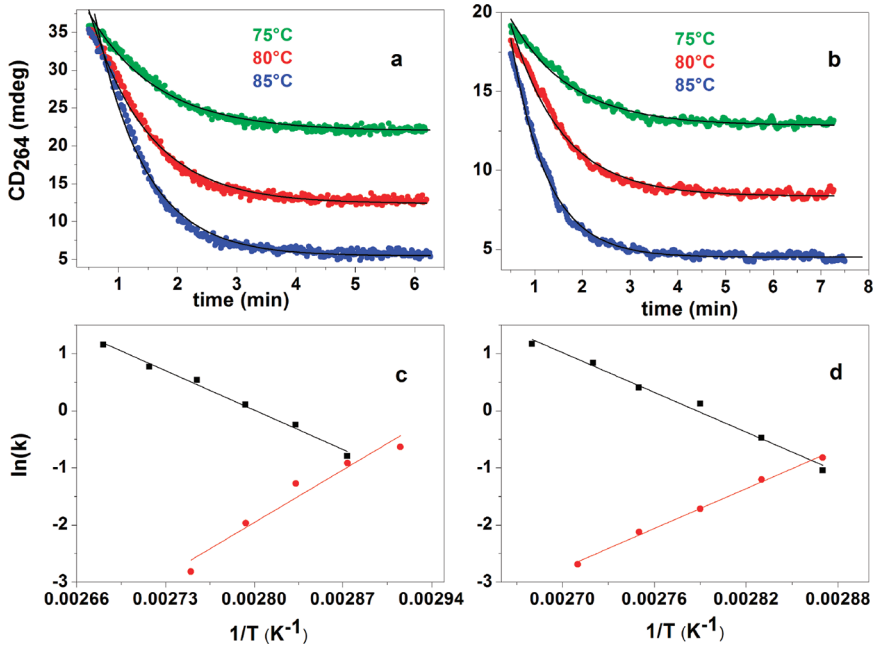

Figure 5. CD intensity at 264 nm as a function of time at three different temperatures for $(TTAGGG)_4TT$ (a) and $(TTAGGG)_8TT$ (b). Arrhenius plots for the P-to-S (black squares) and S-to-P (red circles) reactions for $(TTAGGG)_4TT$ (c) and $(TTAGGG)_8TT$ (d). All the solutions contain 20 mM phosphate with 100 mM KCl, 0.1 mM EDTA, 40% PEG200, at pH 7.0. The DNA concentrations were 48 and 20 μM for $(TTAGGG)_4TT$ and $(TTAGGG)_8TT$, respectively.

dx.doi.org/10.1021/jp209170v | J. Phys. Chem. B 2012, 116, 2294–2305

Table 3. Kinetic Parameters for the P-to-S and S-to-P Reactions

T (°C)	k_2 (min^{-1})	k_{-2} (min^{-1})	E_a^{2} (kJ mol^{-1})	E_a^{-2} (kJ mol^{-1})	$\Delta H^{0\,a}$ (kJ mol^{-1})
			$(TTAGGG)_4TT$		
70	0.19 ± 0.06	0.53 ± 0.05			
75	0.45 ± 0.06	0.40 ± 0.08			
80	0.78 ± 0.08	0.28 ± 0.07			
85	1.11 ± 0.07	0.14 ± 0.06	82 ± 4	−98 ± 12	180 ± 13
90	1.71 ± 0.08	0.06 ± 0.05			
95	2.15 ± 0.09	0.03 ± 0.02			
100	3.18 ± 0.08	n.d.			
			$(TTAGGG)_8TT$		
75	0.35 ± 0.08	0.44 ± 0.05			
80	0.62 ± 0.06	0.30 ± 0.06			
85	1.13 ± 0.06	0.19 ± 0.04			
90	1.5 ± 0.1	0.12 ± 0.07	94 ± 6	−91 ± 4	185 ± 7
95	2.3 ± 0.2	0.07 ± 0.05			
100	3.2 ± 0.2	n.d.			

[a] Computed from $\Delta H^0 = E_a^{2} - E_a^{-2}$.

these considerations, we performed the kinetic experiments in the range 70−100 °C, assuming that, in this temperature range, only the P−S and the S−P reactions contribute to the CD signal variation at 264 nm. Before each kinetic experiment, the samples were equilibrated at 60 °C to start from the maximum of the parallel conformation. Figure 5 shows the behavior of the CD signal at 264 nm with increasing time at three different temperatures for $(TTAGGG)_4TT$ and $(TTAGGG)_8TT$. The kinetic parameters were obtained by fitting the experimental kinetic curves with eq 5 (see Experimental Methods).

There was good agreement between the fitting and the experimental kinetic curves for both $(TTAGGG)_4TT$ and $(TTAGGG)_8TT$. The corresponding Arrhenius plots are shown in Figure 5c,d, and the obtained kinetic parameters are reported in Table 3. We found a negative activation energy for the S−P conversion, revealing that this process cannot be described with an elementary reaction but involves a more complex kinetic mechanism. This result is consistent with reported data showing that intermediate species are involved in the formation of a human telomeric quadruplex from an unfolded single strand.[30,39−41] The activation energy for the P-to-S transition is greater for $(TTAGGG)_8TT$ compared to $(TTAGGG)_4TT$, suggesting that the conformational change of each subunit in the $(TTAGGG)_8TT$ parallel structure is affected by the presence of the other quadruplex subunit (Table 3). This result is consistent with the suggested model for an all-parallel multimer[42] involving additional stacking interactions between the G-tetrad cores of the two adjacent parallel quadruplex subunits.

The k_{-2} value for $(TTAGGG)_4TT$, extrapolated at 37 °C, is 24.5 min^{-1}, which corresponds to a half-transformation time of about 1.7 s, whereas the reported half-transformation time for the folding of the hybrid conformation is in the milliseconds time range.[29,41] Considering that the hybrid conformation is converted in the parallel conformation very slowly (half-transformation time ∼2.5 h), the much faster folding kinetics of the hybrid quadruplex compared with the parallel quadruplex could be the key factor in determining the biologically relevant quadruplex conformation on the time scale of the biological process, as recently suggested by other authors.[29] The extrapolated k_{-2} value at 37 °C for $(TTAGGG)_8TT$ is 20.5 min^{-1}; this value corresponds to a half-trasformation time of about 2 s. The comparison between the kinetic constants of the two DNA sequences reveals that the presence of consecutive quadruplex units along the same strand has little or no effect on the folding rate of each quadruplex.

Simulation of the CD Variation for the Quadruplex−Quadruplex Interconversion and Unfolding Process and Comparison with the Experimental Data. To get more information on the variation of the relative populations of the different human telomeric DNA conformations, we simulated the whole melting/unfolding process of the human telomeric DNA using our experimental kinetic constants. According to the Scheme 1, at each temperature, the variation of the relative populations of the Hy, P, and S conformations on changing temperature is given by the following set of differential equations:

$$\frac{d\alpha_{Hy}}{dt} = -k_1\alpha_{Hy} + k_{-1}\alpha_P$$

$$\frac{d\alpha_P}{dt} = k_1\alpha_{Hy} - k_2\alpha_P - k_{-1}\alpha_P + k_{-2}(1 - \alpha_{Hy} - \alpha_P) \quad (8-9)$$

where α_i represents the molar fraction of the i species and k_i is the kinetic constant calculated by means of the experimentally determined kinetic parameters (Tables 2 and 3). Considering the relation

$$\frac{d\alpha_i}{dt} = \frac{d\alpha_i}{dT} \times \frac{dT}{dt} \quad (10)$$

the system of differential eqs 8−9 can be rewritten as follows:

$$\frac{d\alpha_{Hy}}{dT} = \left(\frac{dT}{dt}\right)^{-1}(-k_1\alpha_{Hy} + k_{-1}\alpha_P)$$

$$\frac{d\alpha_P}{dT} = \left(\frac{dT}{dt}\right)^{-1}[k_1\alpha_{Hy} - k_2\alpha_P - k_{-1}\alpha_P + k_{-2}(1 - \alpha_{Hy} - \alpha_P)] \quad (11-12)$$

where the term (dT/dt) is the heating rate. Solution of the system of differential eqs 11−12 for a given heating rate gives the Hy and P molar fractions from which the single strand molar fraction (α_S) can be computed ($\alpha_S = 1 - \alpha_{Hy} - \alpha_P$). The molar fraction values as a function of temperature were used to

dx.doi.org/10.1021/jp209170v | J. Phys. Chem. B 2012, 116, 2294−2305

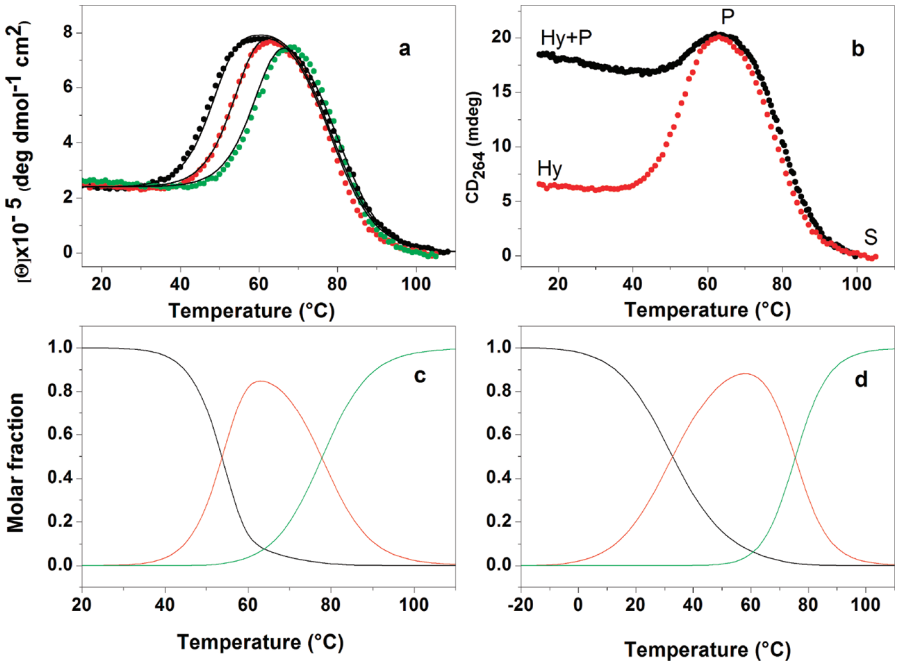

Figure 6. (a) Experimental (colored circles) and simulated (black solid lines) CD melting curves at 264 nm for $(TTAGGG)_4TT$ obtained at 0.3 (black circles), 1.0 (red circles), and 3.0 °C/min (green circles). (b) CD melting curve for $(TTAGGG)_4TT$ of the sample previously equilibrated for 24 h at 37 °C (black) and of the sample just after PEG200 was added (red). The scan rate was 1.0 °C/min. (c) Simulated molar fractions of Hy (black line), P (red line), and S (green line) at a scan rate of 1.0 °C/min and (d) at a scan rate of 0.00001 °C/min for $(TTAGGG)_4TT$. The DNA concentration was 30 μM.

compute the expected CD melting plots at 264 nm by means of the following equation:

$$[\Theta]_{264nm} = [\Theta]^{Hy}_{264nm} \times \alpha_{Hy} + [\Theta]^{P}_{264nm} \times \alpha_{P} + [\Theta]^{S}_{264nm} \times \alpha_{S} \quad (13)$$

where $[\Theta]^{Hy}_{264nm}$ is the molar ellipticity at 264 nm before heating the sample ($\alpha_{Hy} = 1$) and can be experimentally measured; $[\Theta]^{P}_{264nm}$ is the molar ellipticity at 264 nm when ($\alpha_P = 1$) all the DNA is in a P fold (we assumed this value equal to the ellipticity measured at 60 °C), whereas $[\Theta]^{S}_{264nm}$ is the ellipticity at 264 nm of the unfolded strand ($\alpha_S = 1$) and can be neglected. Figure 6a shows the comparison between the simulated and experimental CD melting curves obtained for $(TTAGGG)_4TT$ at different scan rates (similar results were obtained with $(TTAGGG)_8TT$). The good agreement between the experimental and simulated curves is a further validation of the experimentally determined, kinetic parameters. The simulation allowed us to plot separately the behavior of each molar fraction on changing temperature.

Figure 6c shows the molar fractions of the three species at a 1.0 °C/min scan rate in the range 20−105 °C. The plot shows an increase of the P molar fraction and a corresponding decrease of the Hy molar fraction in the range 30−60 °C followed by a decrease of the P molar fraction and an increase of the S molar fraction in the range 60−105 °C. Interestingly, the molar fraction of the P conformation does not (at all scan rates simulated) reach unity and to have a good agreement between the experimental and simulated curves we employed in eq 13 a $[\Theta]^{Hy}_{264nm}$ value ~10% greater than the experimental value measured at 60 °C. This observation indicates that the maximum experimental CD value reached at 264 nm (after annealing or after equilibration of the sample at 60 °C) could not be a suitable marker for total Hy−P transformation as supposed in previous studies.[14,16,27] The good agreement between the experimental and simulated curves suggests that the simulated molar fractions well reproduce the conformational populations of the human telomeric DNA. Figure 6d shows the simulated molar fractions for Hy, P, and S at very slow scan rate (0.00001 °C/min) for $(TTAGGG)_4TT$; the corresponding molar fractions can be considered "at thermodynamic equilibrium" and reflect the relative populations of Hy, P, and S under equilibrium conditions. As expected, at equilibrium, the Hy conformation is favored at low temperature as the Hy−P reaction is an endothermic reaction. Both of the quadruplex conformations are significantly populated around physiological temperature. To further prove the existence of the hybrid conformation at 37 °C under equilibrium conditions, we performed the CD melting of the two DNA sequences after equilibration at 37 °C for 24 h. For both DNA sequences, the corresponding melting curves show the characteristic behavior diagnostic of the Hy-to-P transition (over 40 °C), confirming the initial presence of a significant amount of Hy conformation in the starting DNA samples (Figure 6b and Figure S5, Supporting Information).

It should be noted that the CD signal of the parallel conformation is much higher than the CD signal of the hybrid conformation; this fact can affect the estimates of the relative populations of the two conformations based only on a "qualitative" inspection of the spectral shape. To stress this point, we simulated the expected CD spectrum for several mixtures of the two conformations assuming that the 100% hybrid spectrum is given by the initial spectrum of the sample (before heating) and the 100% parallel spectrum is given by the spectrum recorded after equilibration at 60 °C and corrected for this estimated molar fraction. As expected, the simulated spectra (Figure 7) slightly differ from the characteristic spectrum of the parallel fold even in the presence of a

dx.doi.org/10.1021/jp209170v | J. Phys. Chem. B 2012, 116, 2294−2305

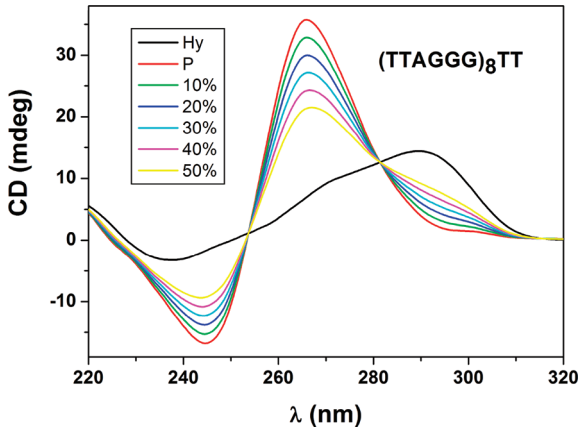

Figure 7. Simulated CD spectrum of $(TTAGGG)_8TT$ for the Hy conformation (black line), the P conformation (red line), and for mixtures of different concentrations of Hy and P. In the inset: percent of DNA in the Hy conformation.

significant amount of hybrid-type conformation (up to 30–40%).

Gel Electrophoresis Confirms the Coexistence of the Hy and P Conformations in the Telomeric DNA Equilibrated at 37 °C. The PEG-induced conformational conversion of $(TTAGGG)_4TT$ and $(TTAGGG)_8TT$ quadruplex forming sequences was also examined by following native gel electrophoreses. In these experiments, quadruplex samples (lanes 1–3) were prepared in 100 mM K^+ solution, by heating at 90 °C for 5 min, and then slowly cooled to room temperature. Next, PEG200 was added to 40% (w/v) for the respective measurements under the appropriate conditions (see legend of Figure 8). Previous studies of the human telomeric

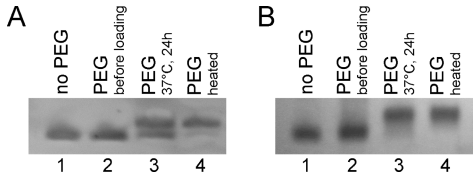

Figure 8. Gel electrophoresis analysis of intramolecular folding of $(TTAGGG)_4TT$ (A) and $(TTAGGG)_8TT$ (B) quadruplexes induced by 40% (w/v) PEG200 in 100 mM K^+ solution. The sample of lane 1 was loaded into the gel without treating with PEG. The samples of lanes 2–4 were prepared in the presence of PEG: the sample of lane 2 was mixed with PEG just before loading onto the gel; the sample of lane 3 was loaded after bathing at 37 °C for 24 h before electrophoresis; the sample of lane 4 was heat denatured and renatured in the presence of PEG.

DNA in K^+/PEG solution revealed that it adopts a parallel-stranded conformation characterized by a slower migration band in gel electrophoresis compared to the hybrid structure, with faster migration, adopted in K^+ solution.[14,27] In agreement with these studies, our electrophoreses (Figure 8) show that the K^+/PEG parallel-stranded quadruplex (lane 4), prepared by heat denaturation and renaturation of the samples in K^+/PEG solution, is less compact than the hybrid-type K^+-quadruplex (lane 1) for both $(TTAGGG)_4TT$ and $(TTAGGG)_8TT$ (Figure 8A and B, respectively). Thus, we used their mobility as a reference for monitoring the composition of the DNA samples equilibrated at 37 °C for 24 h (lane 3). For the $(TTAGGG)_4TT$ single quadruplex, we clearly observed two bands (lane 3, Figure 8A) having similar shapes/mobilities to that of the hybrid and parallel quadruplex for the faster and slower migrating band, respectively. Gel quantitative analysis reveals that the Hy concentration in the equilibrated sample at 37 °C is about 40%. For the $(TTAGGG)_8TT$ two-quadruplex-forming sequence, the band corresponding to the hybrid conformation is still present (lane 3, Figure 8B) but less marked, suggesting that the presence of two consecutive quadruplex subunits favors the parallel folding in comparison with the $(TTAGGG)_4TT$ single quadruplex. This result is consistent with the data of Table 2, indicating that the parallel fold is favored for $(TTAGGG)_8TT$ in comparison with $(TTAGGG)_4TT$. This result suggests that the Hy–P interconversion of each quadruplex subunit in $(TTAGGG)_8TT$ is affected by the presence of the adjacent quadruplex and reveals a cooperative effect between the two subunits during the Hy-to-P reaction. This effect could be justified on the basis of the proposed model for the $(TTAGGG)_8TT$ parallel structure. In that model, extensive stacking interactions are present between the terminal G-tetrads of two parallel quadruplex subunits.[42] To maximize these interactions, the two quadruplex subunits need to both be parallel; thus, it is likely that the folding of one subunit in the parallel form induces cooperatively the Hy–P transition in the other quadruplex subunit.

The Degree of Hy–P Interconversion Depends on the Nature of the "Crowding Agent". In order to explore the mechanism of the conformational conversion induced by the crowding agent, we employed PEG of different molecular weights (3400 and 10000 Da) as well as crowding agents of different nature as the polysaccharide Ficoll 400 and glycerol. The results of the Hy–P interconversion kinetic experiments at 37 °C in the different crowding agents are summarized in Table 4. On increasing the PEG molecular weight, the Hy-to-P

Table 4. Kinetic and Equilibrium Constants for the Hy–P Interconversion at 37 °C in the Presence of 40% (w/v) of Different Crowding Agents

crowding agent	k_1 (min^{-1})	k_{-1} (min^{-1})	K_{eq} [a]
	$(TTAGGG)_4TT$		
PEG200	$(4.6 \pm 0.2) \times 10^{-3}$	$(3.0 \pm 0.1) \times 10^{-3}$	1.5 ± 0.1
PEG3400	$(1.2 \pm 0.1) \times 10^{-3}$	$(4.1 \pm 0.1) \times 10^{-3}$	0.3 ± 0.1
PEG10000	$(2.1 \pm 0.1) \times 10^{-3}$	$(1.2 \pm 0.1) \times 10^{-2}$	0.2 ± 0.1
glycerol[b]	n.d.	n.d.	~0
Ficoll400[b]	n.d.	n.d.	~0
	$(TTAGGG)_8TT$		
PEG200	$(6.4 \pm 0.2) \times 10^{-3}$	$(2.9 \pm 0.1) \times 10^{-3}$	2.2 ± 0.1
PEG3400	$(2.7 \pm 0.1) \times 10^{-3}$	$(7.3 \pm 0.1) \times 10^{-3}$	0.4 ± 0.1
PEG10000	$(2.1 \pm 0.1) \times 10^{-3}$	$(1.1 \pm 0.1) \times 10^{-2}$	0.2 ± 0.1
glycerol[b]	n.d.	n.d.	~0
Ficoll400[b]	n.d.	n.d.	~0

[a] Computed from $K_{eq} = k_1/k_{-1}$. [b] No Hy-to-P transition was observed for the DNA equilibrated at 37 °C for 24 h.

interconversion rate decreases and the P-to-Hy rate increases, resulting in a decrease of the equilibrium constant (k_1/k_{-1}) for the Hy–P reaction. Particularly, for PEG3400 and PEG10000, we found that the Hy is the dominant conformation at equilibrium ($K_{eq} < 1$), whereas, for PEG200, the P form is dominant ($K_{eq} > 1$). This observation could be explained by assuming that the presence of PEG stabilizes the parallel conformation by lowering the water activity, as previously

dx.doi.org/10.1021/jp209170v | J. Phys. Chem. B 2012, 116, 2294–2305

suggested.[21] Indeed, considering the differences in molecular mass between PEG200, PEG3400, and PEG10000, their 40% (w/v) solutions are characterized by different molar concentrations ([PEG200] = 2 M, [PEG3400] = 0.1 M, [PEG10000] = 0.04 M]) and, hence, different water activities. Particularly, the water activity will be lower in the 40% (w/v) PEG200 buffer in comparison with the 40% (w/v) PEG3400 or PEG10000 buffers. In conclusion, the observed decrease of the stability of the parallel quadruplex on increasing PEG molecular weight could be justified by the related increase of the water activity.

Interestingly, we did not observe Hy-to-P transition for both DNAs (incubated at 37 °C up to 24 h) with Ficoll 400 or glycerol as crowding agents (Table 4). The interconversion was not observed also after heating at 90 °C and slow cooling of the samples (data not shown). These results indicate that the hybrid forms are stable when Ficoll 400 or glycerol are employed as the crowding agent; similar results have been previously observed with Ficoll 70.[19] Interestingly, this observation was not expected for glycerol on the basis of its effect on water activity. Indeed, the buffer containing glycerol should have the lowest water activity among the studied buffers and consequently should stabilize the parallel quadruplex. On the contrary, the observed stabilization of the hybrid conformation strongly suggests that glycerol affects the Hy−P transition with a different mechanism. Although further studies are needed to clarify this behavior, a tentative explanation could be the presence of a direct solvation of the DNA quadruplexes by this cosolute with a higher number of hydroxyl groups, thus balancing the decrease of the water activity. In other words, the solvation of nucleotides by glycerol molecules could eliminate the release of water molecules involved in the Hy−P transition.

CONCLUSIONS

Human telomeric DNA is highly polymorphic, and the knowledge of which conformation is favored in physiological conditions is extremely important. Many previous studies have emphasized that several G-quadruplex conformations convert in the parallel quadruplex structure under a crowded, cell-like environment, simulated by PEG. In this study, we showed that the parallel conformation is not the only populated conformation in the presence of PEG but a significant amount of hybrid quadruplex coexists with the parallel quadruplex. Further, folding kinetic parameters extrapolated at physiological temperature suggest that telomeric DNA folds in the parallel quadruplex in the seconds time scale, a much larger time scale than the one reported for the hybrid quadruplex folding (∼ms). Comparing the $(TTAGGG)_4TT$ and $(TTAGGG)_8TT$ sequences, we found that the presence of consecutive quadruplex subunits slightly favors the parallel fold and affects the P-to-S transition as revealed by the higher activation energy for $(TTAGGG)_8TT$ compared to $(TTAGGG)_4TT$. This observation could be justified on the basis of the proposed model for the $(TTAGGG)_8TT$ parallel structure involving extensive stacking interactions between the G-tetrad cores of the two adjacent parallel quadruplex subunits.[42] On the other hand, analysis of the S−P kinetic parameters revealed that the presence of consecutive quadruplex units along the same strand has little or no effect on the folding rate of each quadruplex subunit. In conclusion, the whole of our data suggests that human telomeric DNA is in equilibrium between the hybrid and parallel conformations in PEG containing solution and is even the major conformation in other crowding agents like Ficoll 400 and glycerol. This result is biologically relevant, as it strongly suggests that the hybrid quadruplex is significantly populated under physiological conditions and can be considered as a target structure for drug design. Exploring the thermodynamic coupling of binding reactions of other biological macromolecules or small ligands to these conformational transitions could be the next step to understand and manipulate the telomere biology.

ASSOCIATED CONTENT

Supporting Information

Supplementary CD spectra versus temperature and versus time, table of SVD results, and Arrhenius plots. This material is available free of charge via the Internet at http://pubs.acs.org.

AUTHOR INFORMATION

Corresponding Author

*Phone: +39-081-674263. Fax: +39-081-674090. E-mail: luigi.petraccone@unina.it.

Notes

The authors declare no competing financial interest.

ACKNOWLEDGMENTS

This research was funded by the "Associazione Italiana per la Ricerca sul Cancro" (A.I.R.C. Project No. 6255) and by the COST Action MP0802.

REFERENCES

(1) Blackburn, E. H. *Cell* **2001**, *106*, 661.
(2) Makarov, V. L.; Hirose, Y.; Langmore, J. P. *Cell* **1997**, *88*, 657.
(3) Neidle, S.; Parkinson, G. N. *Curr. Opin. Struct. Biol.* **2003**, *13*, 275.
(4) Neidle, S. *FEBS J.* **2010**, *277*, 1118.
(5) Zahler, A. M.; Williamson, J. R.; Cech, T. R.; Prescott, D. M. *Nature* **1991**, *350*, 718.
(6) Ou, T. M.; Lu, Y. J.; Tan, J. H.; Huang, Z. S.; Wong, K. Y.; Gu, L. Q. *ChemMedChem* **2008**, *3*, 690.
(7) Phan, A. T. *FEBS J.* **2010**, *277*, 1107.
(8) Dai, J.; Carver, M.; Yang, D. *Biochimie* **2008**, *90*, 1172.
(9) Ambrus, A.; Chen, D.; Dai, J.; Bialis, T.; Jones, R. A.; Yang, D. *Nucleic Acids Res.* **2006**, *34*, 2723.
(10) Dai, J.; Carver, M.; Punchihewa, C.; Jones, R. A.; Yang, D. *Nucleic Acids Res.* **2007**, *35*, 4927.
(11) Lim, K. W.; Amrane, S.; Bouaziz, S.; Xu, W.; Mu, Y.; Patel, D. J.; Luu, K. N.; Phan, A. T. *J. Am. Chem. Soc.* **2009**, *131*, 4301.
(12) Parkinson, G. N.; Lee, M. P.; Neidle, S. *Nature* **2002**, *417*, 876.
(13) Li, J.; Correia, J. J.; Wang, L.; Trent, J. O.; Chaires, J. B. *Nucleic Acids Res.* **2005**, *33*, 4649.
(14) Xue, Y.; Kan, Z. Y.; Wang, Q.; Yao, Y.; Liu, J.; Hao, Y. H.; Tan, Z. *J. Am. Chem. Soc.* **2007**, *129*, 11185.
(15) Zhou, J.; Wei, C.; Jia, G.; Wang, X.; Feng, Z.; Li, C. *Biochimie* **2009**, *91*, 1104.
(16) Heddi, B.; Phan, A. T. *J. Am. Chem. Soc.* **2011**, *133*, 9824.
(17) Zhou, J.; Wei, C.; Jia, G.; Wang, X.; Tang, Q.; Feng, Z.; Li, C. *Biophys. Chem.* **2008**, *136*, 124.
(18) Minton, A. P. *J. Biol. Chem.* **2001**, *276*, 10577.
(19) Hansel, R.; Lohr, F.; Foldynova-Trantirkova, S.; Bamberg, E.; Trantirek, L.; Dotsch, V. *Nucleic Acids Res.* **2011**, *39*, 5768.
(20) Zhou, H. X.; Rivas, G.; Minton, A. P. *Annu. Rev. Biophys.* **2008**, *37*, 375.
(21) Miller, M. C.; Buscaglia, R.; Chaires, J. B.; Lane, A. N.; Trent, J. O. *J. Am. Chem. Soc.* **2010**, *132*, 17105.
(22) Miyoshi, D.; Nakao, A.; Sugimoto, N. *Biochemistry* **2002**, *41*, 15017.
(23) Zhang, D. H.; Fujimoto, T.; Saxena, S.; Yu, H. Q.; Miyoshi, D.; Sugimoto, N. *Biochemistry* **2010**, *49*, 4554.

(24) Petraccone, L.; Garbett, N. C.; Chaires, J. B.; Trent, J. O. *Biopolymers* **2010**, *93*, 533.
(25) Cummaro, A.; Fotticchia, I.; Franceschin, M.; Giancola, C.; Petraccone, L. *Biochimie* **2011**, *93*, 1392.
(26) Xu, Y.; Ishizuka, T.; Kurabayashi, K.; Komiyama, M. *Angew. Chem., Int. Ed. Engl.* **2009**, *48*, 7833.
(27) Xu, L.; Feng, S.; Zhou, X. *Chem. Commun. (Cambridge, U. K.)* **2011**, *47*, 3517.
(28) Petraccone, L.; Trent, J. O.; Chaires, J. B. *J. Am. Chem. Soc.* **2008**, *130*, 16530.
(29) Xue, Y.; Liu, J. Q.; Zheng, K. W.; Kan, Z. Y.; Hao, Y. H.; Tan, Z. *Angew. Chem., Int. Ed.* **2011**, *50*, 8046.
(30) Gray, R. D.; Chaires, J. B. *Nucleic Acids Res.* **2008**, *36*, 4191.
(31) Cantor, C. R.; Warshaw, M. M.; Shapiro, H. *Biopolymers* **1970**, *9*, 1059.
(32) Lieberman, D. V.; Hardin, C. C. *Biochim. Biophys. Acta* **2004**, *1679*, 59.
(33) Gray, R. D.; Chaires, J. B. In *Current Protocols in Nucleic Acid Chemistry*; Wiley: New York, 2011; Chapter 17, Unit 17.4.
(34) Hendler, R. W.; Shrager, R. I. *J. Biochem. Biophys. Methods* **1994**, *28*, 1.
(35) Petraccone, L.; Pagano, B.; Esposito, V.; Randazzo, A.; Piccialli, G.; Barone, G.; Mattia, C. A.; Giancola, C. *J. Am. Chem. Soc.* **2005**, *127*, 16215.
(36) Haq, I.; Chowdhry, B. Z.; Chaires, J. B. *Eur. Biophys. J.* **1997**, *26*, 419.
(37) Zhang, D. H.; Fujimoto, T.; Saxena, S.; Yu, H. Q.; Miyoshi, D.; Sugimoto, N. *Biochemistry* **2010**, *49*, 4554.
(38) Lim, K. W.; Lacroix, L.; Yue, D. J.; Lim, J. K.; Lim, J. M.; Phan, A. T. *J. Am. Chem. Soc.* **2010**, *132*, 12331.
(39) Lane, A. N.; Chaires, J. B.; Gray, R. D.; Trent, J. O. *Nucleic Acids Res.* **2008**, *36*, 5482.
(40) Mashimo, T.; Yagi, H.; Sannohe, Y.; Rajendran, A.; Sugiyama, H. *J. Am. Chem. Soc.* **2010**, *132*, 14910.
(41) Gray, R. D.; Petraccone, L.; Trent, J. O.; Chaires, J. B. *Biochemistry* **2010**, *49*, 179.
(42) Haider, S.; Parkinson, G. N.; Neidle, S. *Biophys. J.* **2008**, *95*, 296.